The Impact of Oil Properties on Seawater-in-Oil Emulsion Formation: A Mesocosm Flume Tank Investigation

Wen Ji
New Jersey Institute of Technology
323 Dr. Martin Luther King Jr Blvd, Newark, NJ 07102

Jayanth Yalamanchili
New Jersey Institute of Technology
323 Dr. Martin Luther King Jr Blvd, Newark, NJ 07102

Lin Zhao
ExxonMobil Upstream Research Company
22777 Springwoods Village Pkwy., Houston, TX 77389

Timothy J. Nedwed
ExxonMobil Upstream Research Company
22777 Springwoods Village Pkwy., Houston, TX 77389

Roger C. Prince
Stonybrook Apiary
87 Perryville Rd., Pittstown, NJ 08867

Christoph Aeppli
Bigelow Laboratory for Ocean Sciences
60 Bigelow Dr, East Boothbay, ME 04544

Michel C. Boufadel*
New Jersey Institute of Technology
323 Dr. Martin Luther King Jr Blvd, Newark, NJ 07102
*Corresponding author: Email: boufadel@gmail.com

ABSTRACT

Spilled oil mixed with seawater and entrained water bubbles in an oil slick can potentially form an emulsion. The emulsified oil (*i.e.*, the emulsion) has a significantly increased viscosity, which poses extra challenges to oil spill response. Existing information related to the stability of seawater-in-oil emulsions is based on the behavior of emulsions in small, closed systems (*e.g.* small flasks), and some studies have shown that some emulsified oils that exhibited stable behavior in the lab readily spread into sheen in an uncontaminated open water system. We have constructed a mesocosm scale flume tank equipped with artificial solar lamps, white-cap mixing water jets, Langmuir cell mixing, and two weirs to remove diffuse sheening components. In this case, the oil spreading is designed to be 'infinite' and the oil weathering process is in a mostly 'natural' environment in this 8-meter-long, 0.6-meter-wide, and 0.3-meter-deep flume tank, which is filled with 33 g/kg artificial seawater (Instant Ocean). The system can be operated remotely and monitored through the web. Oil samples were collected at 0 h, 1 h, 6 h, 9 h, 24 h, 48 h, and 72 h to monitor changes in physical-chemical properties such as density, viscosity, interfacial tension, water content, water bubble size distribution, and oxygenates with FTIR, etc. The results, we argue, approach reality and could help establish an oil spill prediction model, as many natural processes were considered and simulated.

Key Words: emulsion, mesocosm, sheen, photo-oxidation, surfactant

INTRODUCTION

Floating oil slicks entrain seawater and bubbles from the water column and can potentially form an emulsion. The emulsified oil (*i.e.*, the emulsion) has a significantly increased viscosity (Boufadel et al. 2019; Hedgpeth et al. 2021; Prince and Lessard 2004), which poses extra challenges to the response techniques.

It is well established that resins and asphaltenes enhance oil emulsion formation and stability (Fingas and Fieldhouse 2006). Asphaltenes form a network structure within a thin oil film that separates approaching water bubbles (Czarnecki et al. 2012). Meanwhile, the surfactant-like polar resins tend to maintain small water droplets (1 – 20 μm) in oil (Fingas 1995; Fingas and Fieldhouse 2012). Other surfactant materials such as organometallics, and nitrogen, sulfur and oxygen (NSO) compounds are also important in preventing water-water coalescence within the emulsion (Payne 1982).

Many abiotic processes play important roles in the emulsification processes, including solar photo-oxidation, mixing energy, sheening, etc. Photo-oxidation happens normally after an oil spill, and fundamentally changes the properties of the oil residue (Aeppli 2022). Hydrocarbons are oxidized to a variety of oxygen-containing products (Overton et al. 1980) which likely have surfactant properties that accelerate the emulsification process and stabilize the formed emulsions (Brandvik and Daling 1991). While the photo-oxidized NSO compounds would have enhanced water solubilities and might be expected to be removed from the thick oil, increased diffusion coefficients as a result of elevated viscosities and specific gravities may prevent these materials from being lost (Payne 1982). Nonetheless, the photo-oxidation happens more extensively in thinner oil slicks (Katz et al. 2022) as sunlight penetrates the oil slick (Ward et al. 2018) and oxygen diffuses (Lichtenthaler et al. 1989), while many lab simulations failed to accomplish this

condition. Freeman and Ward (2022) set up 200 μm oil thickness to study the photo-dissolution apparent quantum yields as a function of wavelengths and photons, which in their case simulated the photooxidation corresponding to 2 – 3 weeks light exposure in Gulf of Mexico in summertime. Sheen leads to the removal of many of the lower molecular weight materials and enhances dissolution and evaporation (Payne 1982). Thicker masses in oil slicks exhibit higher wind resistance and thus higher frictional resistance at the oil water interface compared to the sheen (Zodiatis et al. 2017), which leads to the trail and furthermore, disappearance of sheen (Grose et al. 1979; Ranieri et al. 2013; White et al. 2019). Nonetheless, the spilled oil thickness is normally found around 100 μm or less (Carolis et al. 2012; Leifer et al. 2012; Svejkovsky et al. 2016), though heavily emulsified oil could be more than 200 μm (Daling et al. 2003; French-McCay et al. 2021; OC et al. 2012).

Moreover, challenges remain in terms of the actual behavior of emulsion at sea. For example, the surfactants (*i.e.*, the polar resins and some photo-oxidized products) that are inherently present in a spilled oil remain in the flask in most lab-scale investigations, which would impact the subsequent behavior of the emulsion. While at sea, the surfactants are likely to leave the oil, which impacts the emulsification of and/or the stability of emulsion. In an inter-lab comparison on emulsification processes in different vessels (French-McCay et al. 2022), the viscosity data of the emulsion at various labs showed major differences between wave tank/flume tank simulations and the bench-top scale experiments. This was related to the water content after different time period: though SL Ross and NRCan also used flume tank setups (recirculating or closed), their observed water content differed a lot from those at NJIT as NJIT removed sheen materials continuously – and this difference happened after 6 hrs. Herein, the mesocosm-scale investigation was conducted while simulating multiple natural processes (i.e., artificial solar lamps,

white-cap mixing, Langmuir cell, removing sheen, etc.) during the oil emulsification process, aiming to provide more data points to discern the role of photo-oxidation.

METHODS

The flume tank is located in an indoor lab at the Center for Natural Resources at NJIT (NJ, US). The flume is 8 m long × 0.6 m wide × 0.3 m deep (Figure 1), and a disposable white polyethylene plastic sheet covers the inside wall of the flume tank for easy setup and cleaning between experiments. The tank was filled with artificial seawater (salinity at 33‰, maintained at 15°C by a chiller, using instant ocean sea salt (Pentair Aquatic Eco Systems, Inc., NC, US)) to a water depth of 0.25 m for each experiment. The flume tank is housed in a flame-retardant tent (Item 1) with air filtration via two 0.18 m^3/s fans (Item 2, Vivosun, CA, US) to two 140 lbs activated carbon drums (Item 3, Carbtrol Corporation, CT, US) to prevent odor and contaminant escape. An automated control system (LabVIEW by National Instruments) is designed to control the oil movement, sheening, and white-caps through a control camera (Item 4).

The major components of the mesoscale testing system (illustrated in Fig. 1) are described below:

Sunlight:

Artificial sunlight (Item 5) is generated by two Philips metal halide bulbs (BT56, 1500 W; Grainger, US), placed above the flume to illuminate the whole area of the thick oil slick. The spectrum measured by Flame Spectrometers (Ocean Insight, FL, US) is given in Fig. A1 (the probe was placed on the water surface under one of the bulbs), where the UV range intensity (W/m^2) is comparable to the intensity of natural sunlight (20 – 40 W/m^2 in summer time, and 10 to 30 W/m^2 in winter time (Apell and McNeill 2019; Rezaei et al. 2017; Sichel et al. 2007).

Natural dispersion / disappearance of sheen:

To investigate the role of sheen in the emulsification process, two small chambers at the ends of the flume act as weirs (Detail 6 in Figure 1). As sheen is produced, it overflows the weirs and is removed to simulate the natural dispersion of sheen. A computer-controlled fan system (Detail 7) prevents the thicker oil from overflowing. The overflow water is checked by 2 sump-pumps (Detail 8) which turn on to circulate the contaminated water into the activated carbon water filter drums (Detail 9) and flow to the storage tank (Detail 10).

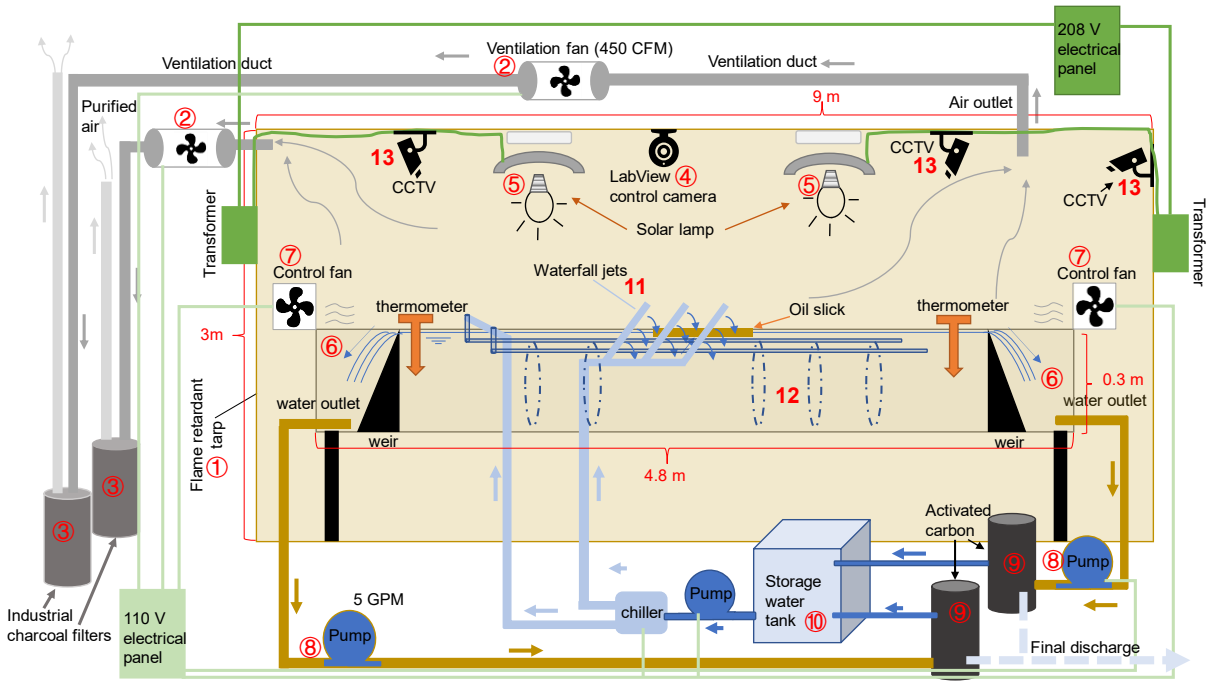

Fig 1. The mesocosm flume tank system simulates seawater-crude oil emulsification process in the ocean, including simulated solar/photo-oxidation, mixing, infinite dilution of sheen, etc. The blue lines represent the clean artificial seawater circulation; the brown lines represent the contaminated seawater circulation; the gray lines represent the air circulation; and the green lines represent the power supplies. The items numbered represent: 1) Flame-retardant tent; 2) ventilation fans; 3) activated carbon air filter drums; 4) LabView control camera; 5) artificial lamps; 6) weir and contaminated water chambers; 7) control fans; 8) sump pumps; 9) activated carbon water filter drums; 10) water storage tank; 11) white-cap mixing (waterfall jets); 12) Langmuir cells; 13) CCTV monitoring cameras.

White-cap mixing:

The mixing was partially contributed by a white-cap-simulation water jet system. The adopted white-cap system consisted of three parallel waterfalls (PVC pipes spraying water at a downward angle of 45° through a series of holes; each waterfall ~50 cm wide, detail 11) placed 5 cm above the water surface across the middle portion of the flume. The waterfall pipes are 0.3 m apart, above the thickest oil slick. White-cap coverage is proportional to the energy dissipation from the wave field (Callaghan 2018; Nissanka and Yapa 2017); white-cap coverage of 1 – 10% indicates an energy dissipation rate of 1 Watt/m^2 (Goddijn-Murphy et al. 2011), which is representative of breaking waves in the field (Chen et al. 2009; Liu et al. 2022). Activation of the spray system is based on signals from the computer-controlled camera that monitors the location of the thick oil slick during the experiments.

Langmuir cells:

Langmuir circulation was first described by Langmuir (1938), who described the phenomenon where buoyant material (e.g., floating bubbles or crude oil) is drawn into bands or `windrows' on the water surface roughly parallel to the direction of the wind. A downward component of motion below the windrows forms at these surface convergences, and surfaces elsewhere (Thorpe 2000), thereby stimulating exchange at the air-oil-seawater interface. A Langmuir cell system (two 4.3 m PVC pipes with holes (Ø 1.59 mm) 2.5 cm apart, pumping water at an upward angle of 45-degree (detail 12) are placed under the water surface along the side walls of the flume (covering about 2/3 of the flume length). The water-flow in the simulated Langmuir cell system is set to be strong enough to generate a surface flow towards the flume center from both flume walls to keep the oil slick thick, while not strong enough to disperse the oil.

Simulation operation:

At the beginning of each experiment, one-liter fresh oil was carefully placed on the water surface, so that when moving from end-to-end, the surface area was controlled at around 0.6 m wide × 6 m long, and the surface thickness was lower than 300 μm, which allows efficient photo-oxidation (Ward et al. 2018). The mesoscale system allows oil and sheen to spread without any boundary (in one dimension) to simulate spreading and sheening of oil in a Langmuir cell in the field. As the sheen developed, one fan was turned on to push the oil and sheen towards a weir. Sheen was allowed to move across the weir to be collected. When LabView detected that the thick oil approached the weir, the first fan was turned off, and the other fan was turned on. This process ran 4 min (LabView controlled time loop), after which both fans were turned on to maintain the oil in the middle of the flume, and the white-cap mixing system was turned on for 10 s. The whole process (oil moving back and forth and the waterfalls) was repeated continuously for 4 days, with continuous operation of the Langmuir cell system. Artificial sunlight was provided during the day (for 8 hours). Additional CCTV (closed-circuit television) cameras (Detail 13) recorded the experiments as needed.

Sample collection:

Samples were taken over time for measurement of bulk properties and composition: 1) water samples were taken from the storage tank every 24 h to examine its surface tension; 2) bulk oil samples were taken at Time = 0 (fresh oil), 1 h, 6 h, 24 h, 48 h, and 72 h for various analyses (see next section) carried out as soon as possible. A stainless-steel spatula was used to scoop up surface oil/emulsion when both fans were turned on to maintain the oil concentrated in the middle; 3) sheen samples were collected at T = 1 h, 6 h, 24 h, 48 h, and 72 h and extracted in dichloromethane (DCM) for various analysis (see next section). The method used a

polytetrafluoroethylene (PTFE/Teflon) membrane to absorb the sheen, and DCM to wash the sample from the membrane to amber bottles. This sampling was conducted when only one fan pushed the oil towards the other end, with sheen preceding the main slick.

Analysis:

The analyses conducted for both bulk oil samples and sheen samples are listed in Table 1.

Table 1. Oil properties measured at various time steps

Properties	**Method / Instrument**	**Bulk oil volume***
Density	Anton Paar DMA 4200 M	< 5 mL
Interfacial tension	Kruss DSA 25s	< 1 mL
Viscosity[$]	Anton Paar MCR 72	< 1 mL
SARA	Iatroscan MK6 TLC-FID	< 1 mL
Water content	Alcohol (Daling et al. 2014)	~ 5 mL
Water bubble size	Leica Microsystems TCS SP8	< 1 mL
Spreading	Pan test (Zhao et al. 2022)	~ 2 mL
FTIR[§]	Agilent Cary 600 series	< 1 mL

***** All tests were for bulk oil samples, except SARA was conducted for both bulk oil and sheen samples
[$] The shear rate for all oil samples was at 100 s^{-1}
[§] FTIR – Fourier Transform Infrared spectroscopy

The oil volume is of importance as samples were collected 5 times (at least 80 mL bulk oil in total) during the 72 h, and with evaporation and sheen-removal, the total oil loss could be significant, so the sampling was designed to be of small volumes to avoid affecting the bulk oil behaviors through the experiment time. The initial oil loading volume could not be large, as otherwise the surface oil would be too thick and would block the penetration of light (Katz et al. 2022).

RESULTS

An experiment with Alaska North Slope oil is shown in Fig 2. The oil slick in the normal spreading period was around 6 m long, and slightly narrower than the tank width (0.6 m), showing a fair spreading and thickness. Fig. 3 shows the bulk oil at various times. After 1 h, the oil was broken up into droplets and separated floating on the surface, with water bubbles entrained in most oil droplets (Fig 3b). After 9 h, water bubbles in the oil phase were of diverse sizes, with obvious large bubbles (around 2 cm) as shown in Fig. 3c. After 24 h, the water bubbles in the oil slick were smaller at less than 1 cm and were more homogeneous (Fig 3d). After 48 h (Fig. 3e), the oil slick was thicker and the entrained water bubbles were smaller and less visible to the naked eye. After 72 h (Fig. 3f), the water bubbles were evenly distributed within the oil slick, causing the oil slick to be brownish and form ‘chocolate mousses’ (Bridie et al. 1980; Clark et al. 2010).

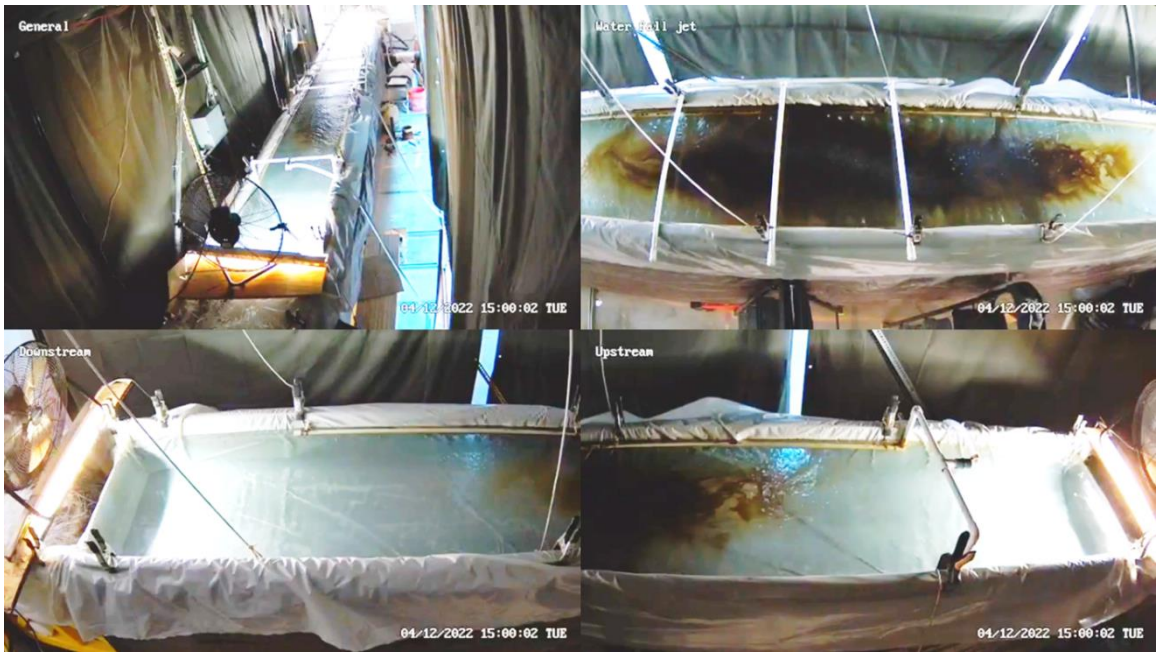

Fig. 2 The photos taken by the CCTV monitoring camera show the movement of surface oil.

The physical properties of the bulk oil at various time steps are reported in Fig. 4. Fig. 4a shows the density of the ANS oil increased from 0.83 g/mL (fresh) to 0.96 g/ml after 72 hours

emulsification simulation, and the viscosity (Fig. 4b) increased from 13 cP (fresh) to >1800 cP. The oil/water interfacial tension (Fig. 4c) increased from 6 mN/m (fresh) to >20 mN/m after 72 h. Fig. 4d shows that the entrained water content increased from 5% to >54% after 72 h. The changes of these physical properties of the bulk oil, as well as visual observations from the CCTV camera system, clearly indicated that the crude oil took up more water bubbles as time passed, and the viscosity, water content, density and interfacial tension all increased.

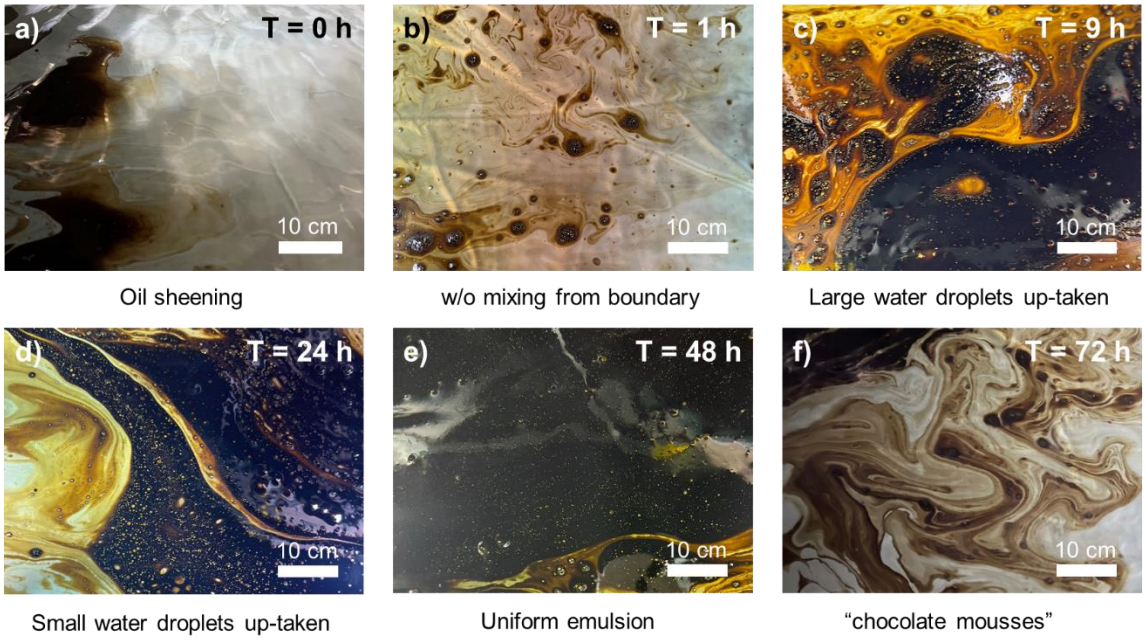

Fig. 3 The photos taken by the CCTV camera showing the surface oil outlook after various durations: a) T=0 h, fresh oil; b) T = 1 h; c) T = 9 h; d) T = 24 h, e) T = 48 h, and f) T = 72 h.

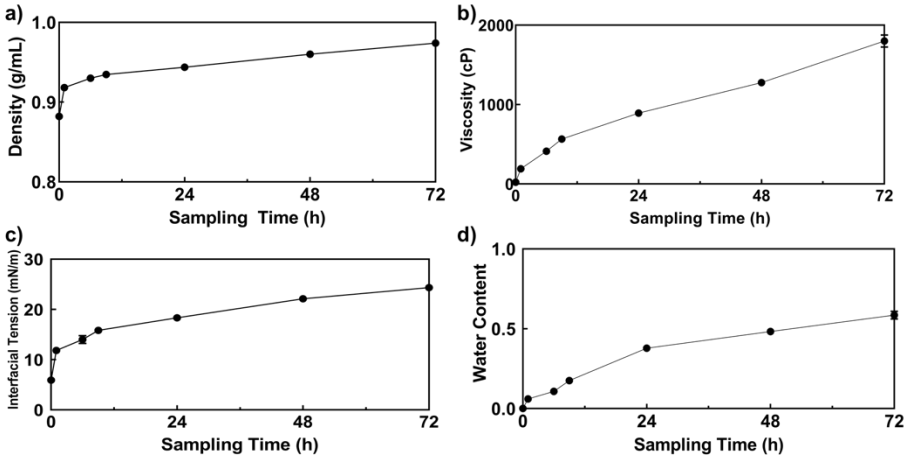

Fig. 4 The physical properties of bulk oil after various durations: a) density; b) viscosity; c) interfacial tension; and d) water content.

Spreading tests were run in a stainless-steel pan covered with a thin PTFE film. The photos in Fig. 5a show that the fresh oil was very dispersive, and after only 20 s there was no obvious oil slick on the water surface. At 9 h, the sample mostly dispersed by 60 s (Fig. 5b), but a few emulsified oil droplets persisted. After 24 h (Fig. 5c) the spreading took longer and there were major oil droplets floating on the surface at 60 s. These droplets diminished after 300 s. At 72 h (Fig. 5d), the emulsified oil droplets there were still droplets entraining water bubbles on the surface at 300 s.

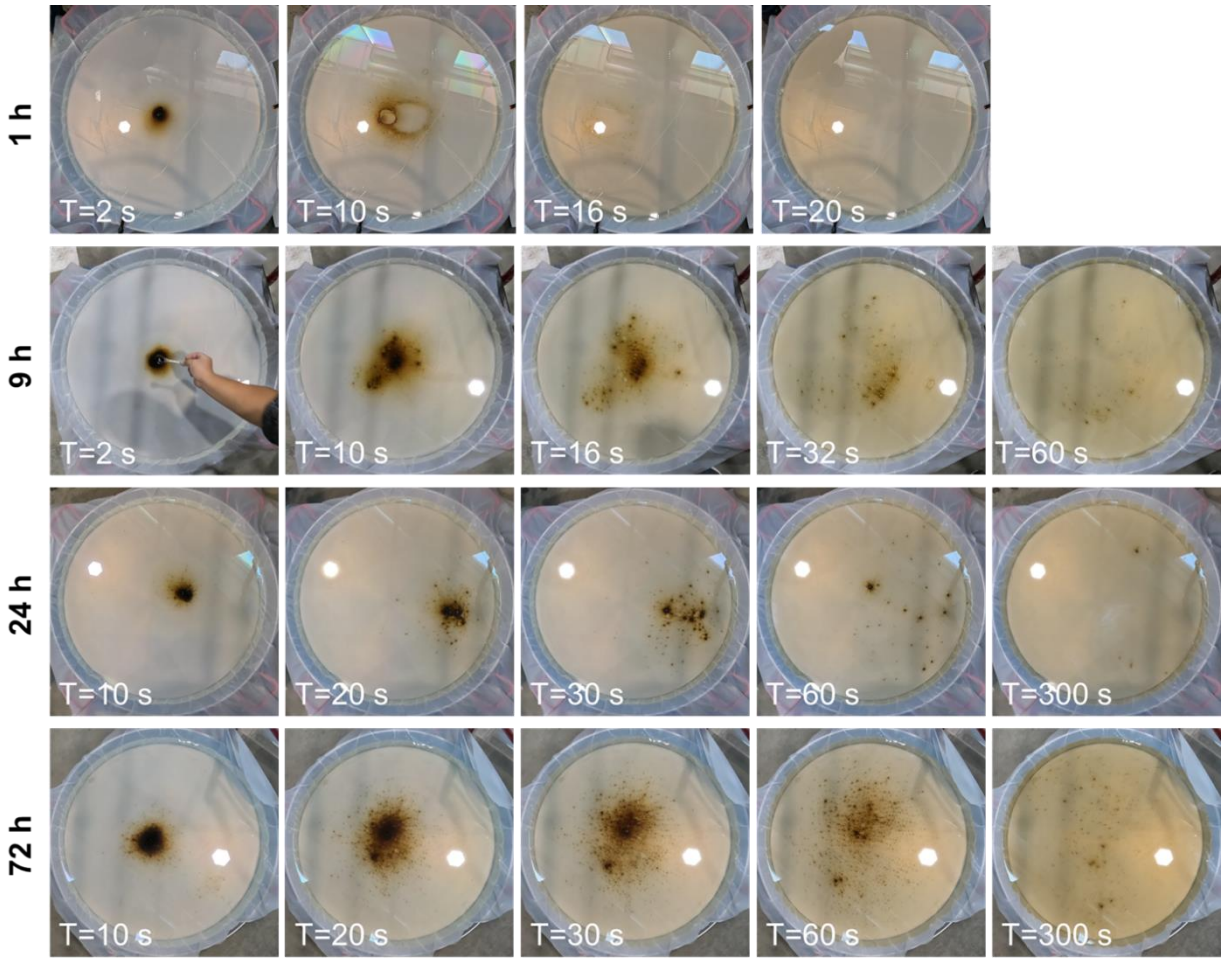

Fig. 5 The spreading tests conducted in a stainless-steel pan for bulk samples after various durations.

The water bubble size distribution results are given in Figs. 6 and A2. After 1 h, the median diameter (d50) was ~35 µm (Fig. 6) and it dropped to ~10 µm after 6 h and 9 h emulsification simulations. After 48 h and 72 h, the d50 increased to 30 µm and 50 µm, respectively. Figure A2 shows that this was likely due to the formation of compound droplets (Muriel and Katz 2021), where crude oil was entrained in water bubbles which were in turn entrained in the oil slick.

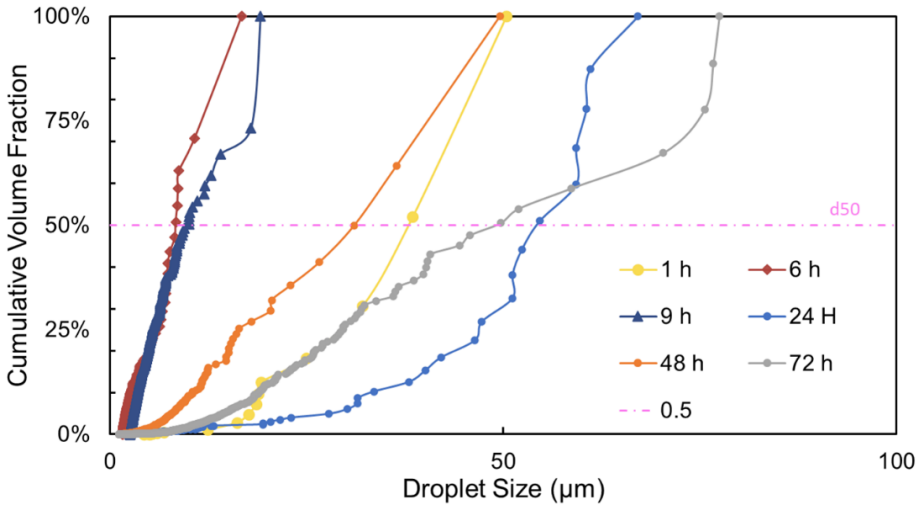

Fig. 6 The water bubble size distribution and the cumulative volume fractions.

The FTIR results are presented in Fig. 7. The photo-oxidation generated typical chemical groups such as the OH stretching band at around 3000 – 3500 cm^{-1} (Boukir et al. 1998; Colthup 2012) and carbonyl groups (diarylketone or quinone structures) at wavenumber 1600 – 1700 cm^{-1} (Boukir et al. 2001)) within 24 hand. These increased by 72 h photo-oxidation and perhaps explain the more stable water-crude oil emulsion at these times; such compounds are more hydrophilic and might act as surfactants (Brandvik and Daling 1991; Lee 1999) to decreased the interfacial tension between crude oil and seawater.

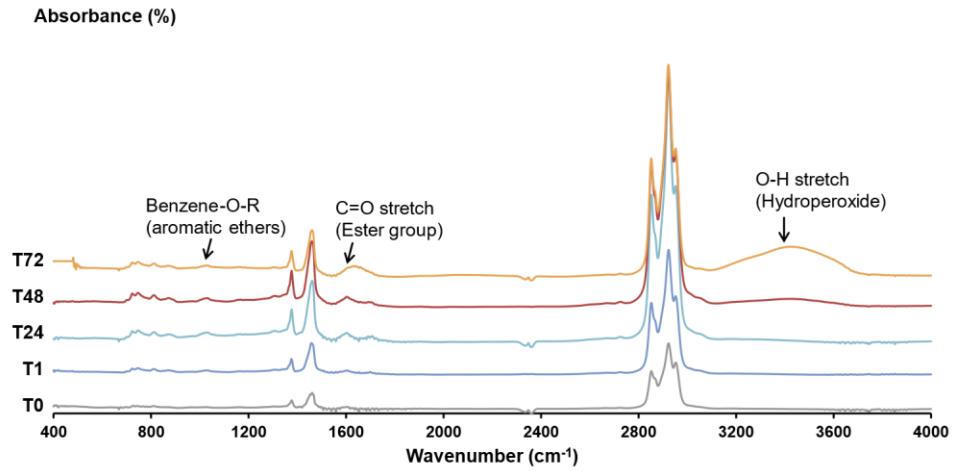

Fig. 7 The FTIR spectra for bulk oil samples.

CONCLUSIONS

The emulsification of Alaskan North Slope (ANS) was studied in a mesocosm scale flume tank equipped with artificial solar lamps, white-cap mixing water jets, Langmuir cell mixing, and two weirs to remove diffused sheening components to simulate the oil emulsification process where spreading is designed to be 'infinite' and the oil weathering process is in a mostly 'natural' environment. The oil became progressively emulsified over 3 days, becoming denser and more viscous as water was incorporated. The water content was over 50% after 3 days under sunlight. The size of entrained water bubbles likely contributed to the increased viscosity, and compound droplets formed with a crude oil in water in crude oil structure. The FTIR spectra showed the addition of oxidized groups, which intensified after longer light exposure. These compounds apparently acted like surfactants to accelerate the emulsification process and stabilize the formed emulsions.

This investigation provided new data points in a mesocosm scale vessel that adopted key abiotic parameters to mimic field conditions, especially including the quantification of photo-oxidation. Further work is needed with additional oils to understand how different oil components (perhaps obtained with SARA) affect the oil emulsification process. In addition, the role of photo-

oxidation and sheening need to be further explored through additional control experiments (dark environment, closed tanks, etc.).

REFERENCES

Aeppli, C. 2022. 'Recent advance in understanding photooxidation of hydrocarbons after oil spills', *Current Opinion in Chemical Engineering*, 36: 100763.

Apell, J. N., and K. McNeill. 2019. 'Updated and validated solar irradiance reference spectra for estimating environmental photodegradation rates', *Environmental science: processes & impacts*, 21: 427-437.

Boufadel, M., X. Geng, C. An, E. Owens, Z. Chen, K. Lee, E. Taylor, and R. C. Prince. 2019. 'A review on the factors affecting the deposition, retention, and biodegradation of oil stranded on beaches and guidelines for designing laboratory experiments', *Current Pollution Reports*, 5: 407-423.

Boukir, A., E. Aries, M. Guiliano, L. Asia, P. Doumenq, and G. Mille. 2001. 'Subfractionation, characterization and photooxidation of crude oil resins', *Chemosphere*, 43: 279-286.

Boukir, A., M. Guiliano, L. Asia, A. El Hallaoui, and G. Mille. 1998. 'A fraction to fraction study of photo-oxidation of BAL 150 crude oil asphaltenes', *Analusis*, 26: 358-364.

Brandvik, P., and P. Daling. 1991. 'W/O-emulsion formation and w/o-emulsion stability testing-an extended study with eight oil types'.

Bridie, A., T. H. Wanders, W. Zegveld, and H. Van Der Heijde. 1980. 'Formation, prevention and breaking of sea water in crude oil emulsions 'chocolate mousses'', *Marine pollution bulletin*, 11: 343-348.

Callaghan, A. H. 2018. 'On the relationship between the energy dissipation rate of surface-breaking waves and oceanic whitecap coverage', *Journal of Physical Oceanography*, 48: 2609-2626.

Carolis, G. D., M. Adamo, and G. Pasquariello. 2012. 'Thickness estimation of marine oil slicks with near-infrared MERIS and MODIS imagery: The Lebanon oil spill case study'. 2012 IEEE International Geoscience and Remote Sensing Symposium. 3002-3005. 10.1109/IGARSS.2012.6350794

Chen, Z., C.-S. Zhan, K. Lee, Z.-K. Li, and M. Boufadel. 2009. 'Modeling oil droplet formation and evolution under breaking waves', *Energy Sources, Part A: Recovery, Utilization, and Environmental Effects*, 31: 438-448.

Clark, R. N., G. A. Swayze, I. Leifer, K. E. Livo, R. Kokaly, T. Hoefen, S. Lundeen, M. Eastwood, R. O. Green, and N. Pearson. 2010. *A method for quantitative mapping of thick oil spills using imaging spectroscopy*. *Vol:* Citeseer

Colthup, N. 2012. *Introduction to infrared and Raman spectroscopy*. *Vol:* Elsevier

Czarnecki, J., P. Tchoukov, and T. Dabros. 2012. 'Possible role of asphaltenes in the stabilization of water-in-crude oil emulsions', *Energy & Fuels*, 26: 5782-5786.

Daling, P. S., F. Leirvik, I. K. Almås, P. J. Brandvik, B. H. Hansen, A. Lewis, and M. Reed. 2014. 'Surface weathering and dispersibility of MC252 crude oil', *Marine pollution bulletin*, 87: 300-310.

Daling, P. S., M. Ø. Moldestad, Ø. Johansen, A. Lewis, and J. Rødal. 2003. 'Norwegian Testing of Emulsion Properties at Sea—The Importance of Oil Type and Release Conditions', *Spill*

Science & Technology Bulletin, 8: 123-136. https://doi.org/10.1016/S1353-2561(03)00016-1.

Fingas, M. 1995. 'Water-in-oil emulsion formation: A review of physics and mathematical modelling', *Spill Science & Technology Bulletin*, 2: 55-59.

Fingas, M., and B. Fieldhouse. 2006. 'A review of knowledge on water-in-oil emulsions'. Proceedings of the Twenty-ninth Arctic and Marine Oilspill Program Technical Seminar, Environment Canada, Ottawa, Ontario. 1-56.

Fingas, M., and B. Fieldhouse. 2012. 'Studies on water-in-oil products from crude oils and petroleum products', *Marine pollution bulletin*, 64: 272-283.

Freeman, D. H., and C. P. Ward. 2022. 'Sunlight-driven dissolution is a major fate of oil at sea', *Science advances*, 8: eabl7605.

French-McCay, D. P., M. Gloekler, R. C. Prince, L. Zhao, T. Nedwed, R. Faragher, B. Hollebone, B. Fieldhouse, Z. Yang, C. Yang, Q. Xin, H. Dettman, D. Cooper, J. McCourt, D. F. Muriel, J. Katz, C. Fuentes-Cabrejo, N. Escobar-Castaneda, K. Stone, A. Guarino, J. Letson, W. Ji, M. C. Boufadel, A. Dhulia, C. Abou Khalil, L.-G. Faksness, P. Daling, C. Aeppli, and C. Barker. 2022. 'Comparison of Laboratory Protocols for Evaluating Oil Emulsification'. 44th AMOP Technical Seminar on Environmental Contamination and Response 2022.

French-McCay, D. P., K. Jayko, Z. Li, M. L. Spaulding, D. Crowley, D. Mendelsohn, M. Horn, T. Isaji, Y. H. Kim, J. Fontenault, and J. J. Rowe. 2021. 'Oil fate and mass balance for the Deepwater Horizon oil spill', *Marine pollution bulletin*, 171: 112681. https://doi.org/10.1016/j.marpolbul.2021.112681.

Goddijn-Murphy, L., D. K. Woolf, and A. H. Callaghan. 2011. 'Parameterizations and algorithms for oceanic whitecap coverage', *Journal of Physical Oceanography*, 41: 742-756.

Grose, P. L., J. S. Mattson, and H. Petersen. 1979. *USNS Potomac oil spill, Melville Bay, Greenland, 5 August 1977: a joint report on the scientific studies and impact assessment*. *Vol:* 79. US Department of Commerce, National Oceanic and Atmospheric Administration

Hedgpeth, B. M., K. M. McFarlin, and R. C. Prince. 2021. 'Crude Oils and their Fate in the Environment', *Petrodiesel Fuels*: 891-910.

Katz, S. D., H. Chen, D. M. Fields, E. C. Beirne, P. Keyes, G. T. Drozd, and C. Aeppli. 2022. 'Changes in Chemical Composition and Copepod Toxicity during Petroleum Photo-oxidation', *Environmental Science & Technology*, 56: 5552-5562.

Langmuir, I. 1938. 'Surface motion of water induced by wind', *Science*, 87: 119-123.

Lee, R. F. 1999. 'Agents which promote and stabilize water-in-oil emulsions', *Spill Science & Technology Bulletin*, 5: 117-126.

Leifer, I., W. J. Lehr, D. Simecek-Beatty, E. Bradley, R. Clark, P. Dennison, Y. Hu, S. Matheson, C. E. Jones, B. Holt, M. Reif, D. A. Roberts, J. Svejkovsky, G. Swayze, and J. Wozencraft. 2012. 'State of the art satellite and airborne marine oil spill remote sensing: Application to the BP Deepwater Horizon oil spill', *Remote Sensing of Environment*, 124: 185-209. https://doi.org/10.1016/j.rse.2012.03.024.

Lichtenthaler, R. G., W. R. Haag, and T. Mill. 1989. 'Photooxidation of probe compounds sensitized by crude oils in toulene and as an oil film on water', *Environmental Science & Technology*, 23: 39-45.

Liu, R., M. C. Boufadel, L. Zhao, T. Nedwed, K. Lee, G. Marcotte, and C. Barker. 2022. 'Oil droplet formation and vertical transport in the upper ocean', *Marine pollution bulletin*, 176: 113451. https://doi.org/10.1016/j.marpolbul.2022.113451.

Muriel, D. F., and J. Katz. 2021. 'Time evolution and effect of dispersant on the morphology and viscosity of water-in-crude-oil emulsions', *Langmuir*, 37: 1725-1742.

Nissanka, I. D., and P. D. Yapa. 2017. 'Oil slicks on water surface: Breakup, coalescence, and droplet formation under breaking waves', *Marine pollution bulletin*, 114: 480-493. https://doi.org/10.1016/j.marpolbul.2016.10.006.

OC, L., U. DE, and P. O. C. RC. 2012. 'OPEN WATER OIL IDENTIFICATION JOB AID'.

Overton, E. B., J. L. Laseter, W. Mascarella, C. Raschke, I. Nuiry, and J. Farrington. 1980. 'Photo-chemical oxidation of IXTOC-I oil'. Proceedings of a Symposium on Preliminary Results from the September 1979 Researcher/Pierce IXTOC I Cruise. Key Biscayne, Florida, June 9–10. 341-383.

Payne, J. R. 1982. 'The chemistry and formation of water-in-oil emulsions and tar balls from the release of petroleum in the marine environment', *Washington: National Academy of Sciences*.

Prince, R. C., and R. R. Lessard. 2004. 'Crude oil releases to the environment: Natural fate and remediation options', *Encyclopedia of Energy*, 1: 727-736.

Ranieri, A., A. P. Lyra, B. Lemos, G. Lutz, and F. Andrade. 2013. 'Oil Spill Response Equipment and Techniques for Waxy Oils in Brazil'. SPE Latin American and Caribbean Health, Safety, Environment, and Sustainability Symposium. SPE-165593-MS.

Rezaei, M., K. Khoshgard, H. Mafakheri, and M. Kanaani. 2017. 'The measurement of solar ultraviolet radiation in Kermanshah city over a one-year period from 2015 to 2016', *International Journal of Radiation Research*, 15: 419-423.

Sichel, C., J. Tello, M. De Cara, and P. Fernández-Ibáñez. 2007. 'Effect of UV solar intensity and dose on the photocatalytic disinfection of bacteria and fungi', *Catalysis Today*, 129: 152-160.

Svejkovsky, J., M. Hess, J. Muskat, T. J. Nedwed, J. McCall, and O. Garcia. 2016. 'Characterization of surface oil thickness distribution patterns observed during the Deepwater Horizon (MC-252) oil spill with aerial and satellite remote sensing', *Marine pollution bulletin*, 110: 162-176. https://doi.org/10.1016/j.marpolbul.2016.06.066.

Thorpe, S. A. 2000. 'Langmuir Circulation and the Dispersion of Oil Spills in Shallow Seas', *Spill Science & Technology Bulletin*, 6: 213-223. https://doi.org/10.1016/S1353-2561(01)00040-8.

Ward, C. P., C. M. Sharpless, D. L. Valentine, D. P. French-McCay, C. Aeppli, H. K. White, R. P. Rodgers, K. M. Gosselin, R. K. Nelson, and C. M. Reddy. 2018. 'Partial photochemical oxidation was a dominant fate of Deepwater Horizon surface oil', *Environmental Science & Technology*, 52: 1797-1805.

White, H. K., C. T. Marx, D. L. Valentine, C. Sharpless, C. Aeppli, K. M. Gosselin, V. Kivenson, R. M. Liu, R. K. Nelson, and S. P. Sylva. 2019. 'Examining inputs of biogenic and oil-derived hydrocarbons in surface waters following the Deepwater Horizon oil spill', *ACS Earth and Space Chemistry*, 3: 1329-1337.

Zhao, L., T. Nedwed, P. S. Daling, and P. J. Brandvik. 2022. 'Investigation of the spreading tendency of emulsified oil slicks on open systems', *Marine pollution bulletin*, 180: 113739.

Zodiatis, G., R. Lardner, T. M. Alves, Y. Krestenitis, L. Perivoliotis, S. Sofianos, and K. Spanoudaki. 2017. 'Oil spill forecasting (prediction)', *Journal of Marine Research*, 75: 923-953.

APPENDIX

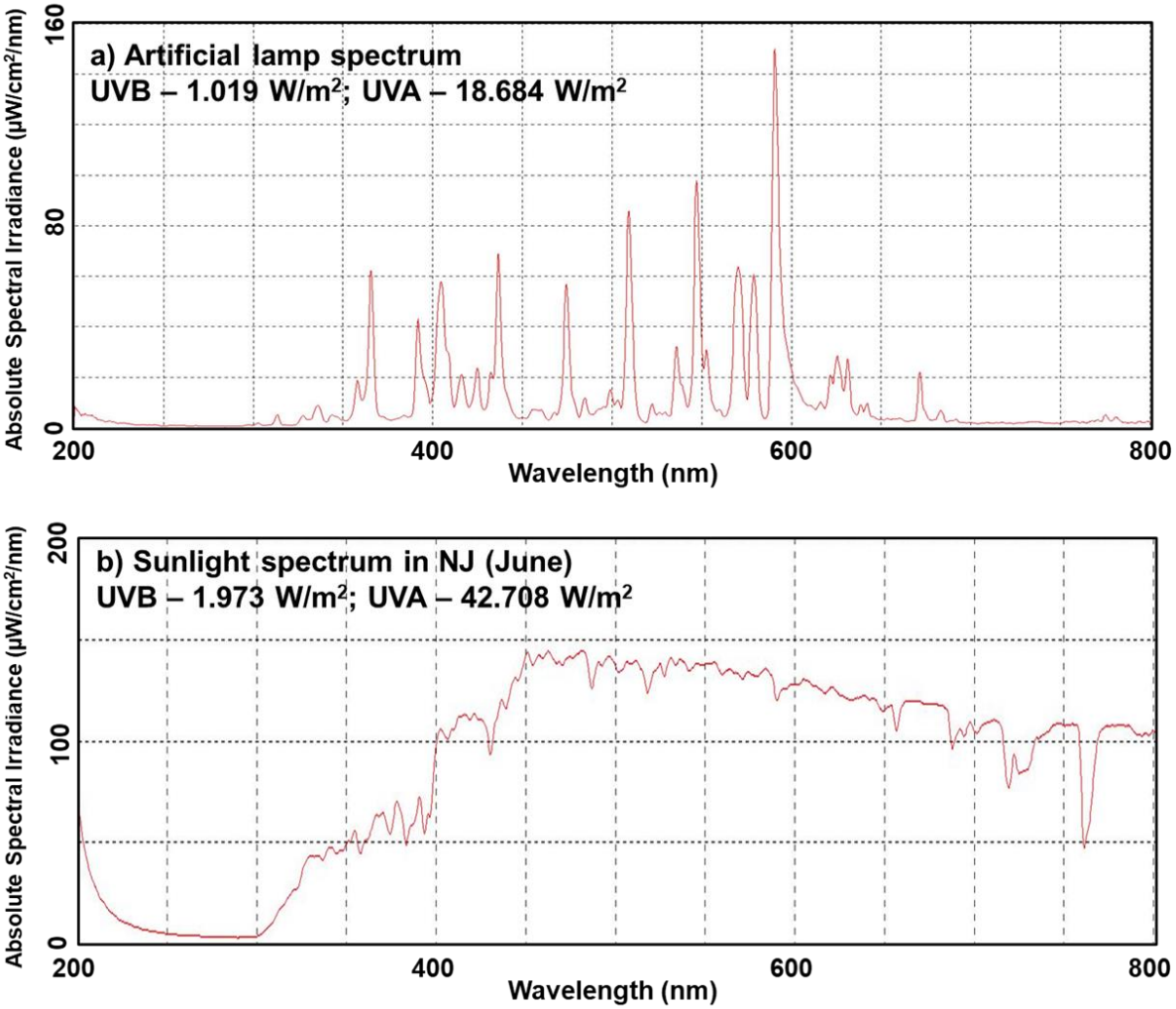

Fig. A1. The solar intensity (and UV intensity) of: a) artificial lamp spectrum and b) natural sunlight at summer noon in NJ. The UVA intensity of artificial sunlight is around 44% of the natural sunlight at summer noon in NJ, and the UVB intensity of the artificial sunlight is around 50% of the natural sunlight at summer noon in NJ. Considering the experiment simulates sunlight exposure in continuous 8 h in one day, the power intensity is comparable.

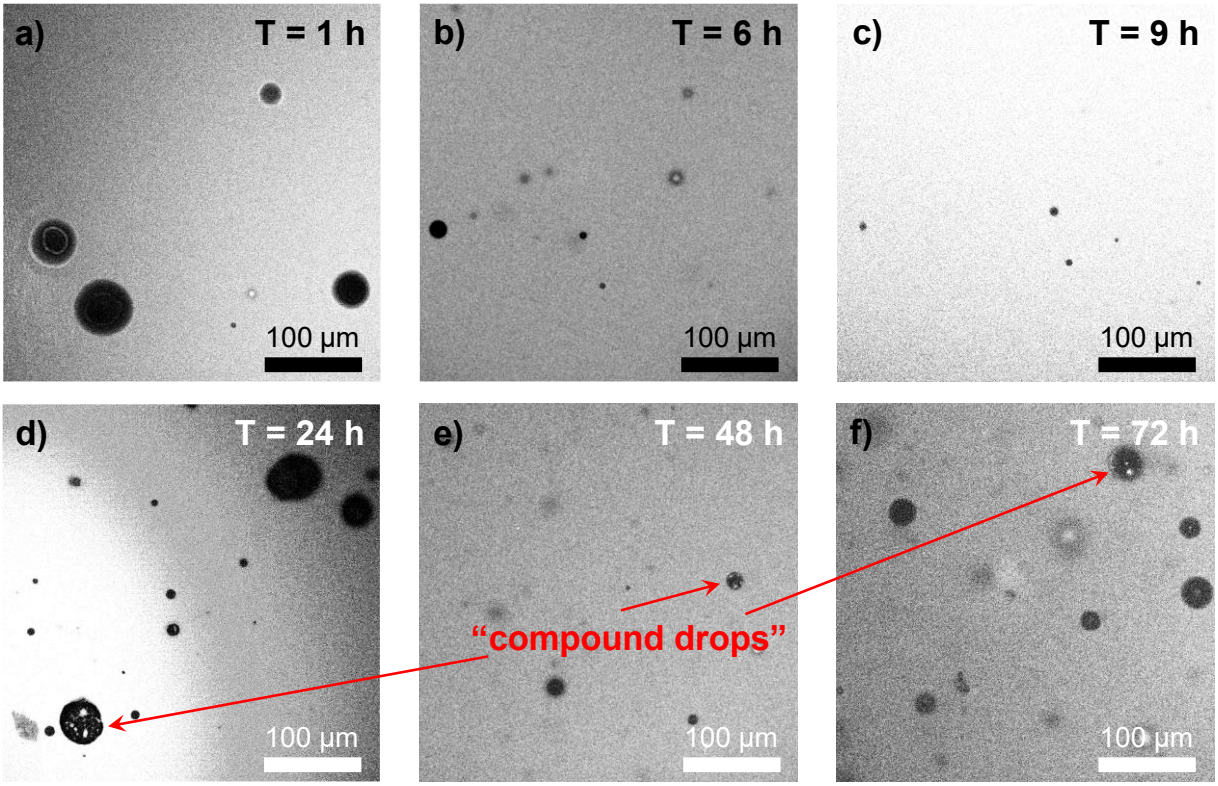

Fig. A2. Microscope photos showing water bubbles entrained in the bulk oil phase after tests ran in: a) 1 h; b) 6 h; c) 9 h; d) 24 h; e) 48 h; and f) 72 h.